

Comparative Analysis of Taper and Taperless Horizontal Turbine Blades at Labuhan Jukung Beach

Setiadi Wira Buana^{1*}, Yudhistira Alghifari Prakoso², Elsa Rizkiya Kencana², Putty Yunesti¹, Wulan Kusuma Wardani¹, Guna Bangun Persada¹, Madi¹

¹ Energy Systems Engineering Study Program, Institut Teknologi Sumatera, Lampung, 35365, Indonesia.

² Ocean Engineering Study Program, Institut Teknologi Sumatera, Lampung, 35365, Indonesia.

* Corresponding Author. E-mail : setiadi.wira@tse.itera.ac.id

Article information - : Received : 23-06-2025; Revised : 09-07-2025; Accepted : 25-06-2025

Abstract

The uneven distribution of electricity demand across Indonesia necessitates the development of Renewable Energy Sources, particularly wind energy. This study evaluates the performance efficiency of horizontal-axis wind turbines equipped with two blade types: taper and taperless, both using the NACA 0012 airfoil. Aerodynamic simulations were conducted using QBlade software. Wind speed data from 2017 to 2022 were sourced from the European Centre for Medium-Range Weather Forecasts (ECMWF), while electricity consumption data were obtained from the Statistics Bureau of Pesisir Barat Regency. A quantitative approach using descriptive graphical analysis was employed to compare the performance metrics of the two blade designs. The results show that the taperless blade achieves higher power coefficient (C_p) and torque coefficient (C_t) values compared to the taper blade, although the taper blade produces greater torque (T). The energy conversion of the taperless blade reached 347.6 kWh, representing an increase of approximately 4.83% over the 331.6 kWh generated by the taper blade. Further analysis indicates that approximately 19 taperless-blade turbines are required to meet the daily electricity demand of 6,545 kWh in Pesisir Barat Regency. These findings support the recommendation to adopt taperless blades for improved wind energy utilization in the region.

Keywords: taper blade; taperless blade; wind energy; NACA 0012.

1. Introduction

The utilization of wind energy potential has become a primary focus as a source of sustainable and environmentally friendly renewable energy. Through the implementation of wind turbines, the kinetic energy from air flow converted into electrical energy can be used to meet public needs. In Indonesia, this potential is increasingly relevant, as harnessing wind energy not only supports the transition to clean energy but also enhances national energy independence and resilience.

Wind turbine is primary device in energy generation systems, with the turbine blades serving as the first components that interact with the wind before it is converted into mechanical energy [1]. Turbine blades affect the performance and efficiency of wind turbines, thereby contributing to their operational stability. The development of innovative blade designs is a crucial factor in improving energy conversion efficiency, particularly under low to moderate wind speed conditions commonly found in tropical regions such as Indonesia. Key design variables such as airfoil shape, blade length, pitch angle, and blade material are central to modern wind turbine research and engineering. By optimizing blade design, previously underutilized wind energy potential can be converted into reliable and sustainable electrical power [2].

Several studies have designed wind turbines with blade types tailored to the characteristics of wind patterns in specific locations, such as coastal or shoreline areas. These blade design adjustments aim to optimize energy conversion efficiency, considering that wind patterns in coastal regions tend to have variable speeds but remain relatively consistent over certain periods [3], [4]. The design adaptations include blade geometry, pitch angle, and the materials used, with the goal of improving turbine efficiency and performance particularly under low to moderate wind conditions commonly found in tropical regions like Indonesia [5]. Previous studies have designed

and evaluated wind turbine blades by considering local geographical characteristics such as coastal and highland regions, utilizing various blade geometries and airfoil types. Tira and Zulfikar [6] developed a taper-type blade using the NACA 24112 airfoil and conducted simulations with QBlade software in Lombok, demonstrating optimal energy conversion efficiency under moderate wind speeds. Akmal et al. [7] investigated taperless blades made of composite materials with the NACA 4412 airfoil, showing superior performance at low wind speeds ranging from 3 to 6 m/s. Wicaksono and Saefudin [8] compared several NACA 4-digit profiles for taperless and untwisted blades, focusing on the lift-to-drag ratio (L/D) as a key indicator of aerodynamic performance. Similarly, Roslan et al. [9] assessed the aerodynamic behavior of small-scale NACA 0012 blades using the blade element momentum theory (BEMT) approach at low wind speeds. However, most of these studies are limited to a single blade geometry or specific operational conditions and lack of a systematic comparison of taper and taperless blades using the same airfoil under tropical low-to-moderate wind environments commonly found in Indonesia. Moreover, there is a notable absence of comprehensive quantitative analyses that evaluate aerodynamic parameters—such as power coefficient (C_p), torque coefficient (C_t), output power (P), and torque (T) in relation to actual electricity consumption in the study area. Therefore, this study aims to address these gaps through a comparative performance analysis based on secondary wind data and numerical simulation.

The selection of Labuhan Jukung Beach, located in Pesisir Barat Regency, Lampung Province, as the research site is based on secondary wind speed data obtained from the European Centre for Medium-Range Weather Forecasts (ECMWF) for the period 2017–2022 [10]. The data indicates that the average wind speed in the area ranges from 2.5 to 6 m/s, which corresponds to Wind Power Class (WPC) 1 to 4 according to the classification by the National Renewable Energy Laboratory (NREL) [11]. This wind speed range is considered suitable for the development of small- to medium-scale wind turbines [12]. Furthermore, the region exhibits a relatively high daily electricity demand, reaching approximately 6,545 kWh based on local government energy consumption reports [13]. Meanwhile, electricity supply from the main grid remains limited and unevenly distributed. These factors position Labuhan Jukung Beach as a promising location for the implementation of wind energy technologies as a sustainable alternative energy solution.

This study employs the NACA 0012 airfoil for both taper and taperless horizontal-axis wind turbine blades due to its symmetrical shape, zero camber, and 12% chord thickness, which ensure stable performance under varying wind directions and speeds [14], [15]. Taper blades feature decreasing chord lengths from root to tip, optimizing performance at higher wind speeds, while taperless blades have constant chord lengths for stable performance at moderate speeds [16]. Both blade types are relevant for the site's wind conditions.

This research contributes to the scientific understanding of the aerodynamic performance differences between taper and taperless blades using the same airfoil under tropical low-to-moderate wind conditions. By systematically analyzing key performance parameters (C_p , C_t , P , T) in relation to tip speed ratio (TSR) and local electricity demand, the study provides valuable insights for optimizing blade design in comparable climatic regions.

Practically, the findings support the development of more efficient wind turbines tailored to Indonesia's unique wind resources, facilitating the integration of renewable energy into the local power grid. The estimation of the optimal number of turbines required to meet regional electricity demand offers guidance for policymakers and engineers in planning sustainable wind energy projects, thereby promoting energy independence and environmental sustainability. Simulations and energy conversion analyses for both blade types are conducted using QBlade software.

2. Experimental Methods

This study was conducted at Labuhan Jukung Beach, located in Pesisir Tengah Subdistrict, Pesisir Barat Regency, Lampung Province. The tools used in this research include QBlade software for wind turbine performance simulation and ArcGIS for mapping the research location. QBlade was selected in this study due to its implementation of the BEMT, which enables accurate aerodynamic performance analysis of wind turbines [17]. Its integration with XFOIL allows for detailed airfoil characterization, making it particularly suitable for simulating wind conditions in low to moderate speed ranges, such as those commonly found in tropical regions [4]. The

research materials consist of secondary data, including wind speed data from 2018 to 2022 obtained from the ECMWF. Electricity consumption data for the Pesisir Tengah Subdistrict sourced from the 2022 Statistics Report by the Central Bureau of Statistics (BPS) of Pesisir Barat Regency. The experimental method involved the simulation of horizontal-axis wind turbines equipped with three blades. Each turbine has a radius of 4 meters and utilizes blades with a chord length of 0.25 meters.

The method used in this study is a quantitative approach with descriptive analysis through graphical visualization. The data are processed to produce clear and informative graphs that present an overall picture of the findings. Comparative graphical data presentation is employed to facilitate the analysis and interpretation of the results. Data collection was carried out by accessing secondary sources online from the official websites of ECMWF and BPS of Pesisir Barat Regency. The obtained wind speed data consist of the u_{10} and v_{10} components at a height of 10 meters, which were analyzed using the total wind speed equation in a two-dimensional orthogonal plane to determine the actual wind speed using following equation [18], [19].

$$V = \sqrt{u^2 + v^2} \quad (1)$$

where u represents the horizontal wind speed component (east-west), v is the vertical wind speed component (north-south), and V is the total or resultant wind speed at a specific height (commonly 10 m).

The next stage of data processing was carried out by inputting wind turbine parameters into the QBlade software. These parameters included energy capacity, system efficiency, turbine radius, and blade characteristics such as the NACA 0012 airfoil type and the number of blades. Simulations were conducted to obtain the relationships between TSR and power coefficient (C_p), thrust coefficient (C_t), torque, and turbine power output. The simulation results were then analyzed to determine the optimal performance of wind turbines using taper and taperless blade configurations at the research location. This analysis served as a foundation for evaluating wind energy potential as a renewable energy source at Labuhan Jukung Beach.

3. Results and Discussion

3.1. Calculation Results and QBlade Simulation

Based on the literature review, the formulation of Parameter 1 as the initial database for the taperless blade design process requires prior calculation of wind speed. This calculation refers to the method outlined in the research methodology section, resulting in the determination of the maximum wind speed (V_{max}), which served as the primary reference in the simulation and design process.

The blade efficiency is set at 40%, in accordance with the theoretical limitation based on the Betz Limit, which states that the maximum efficiency of a wind turbine blade cannot exceed 59.3% [20], [21]. Other components, such as the generator, controller, and transmission, each have an efficiency of 90%, which falls within the typical range for energy conversion systems. The energy consumption data of 6,546 kWh is identified as the annual electricity demand in the Labuhan Jukung Beach area, Pesisir Tengah Subdistrict. Wind energy was estimated by dividing the required electrical output by system efficiency, yielding 2256 kW. Subsequently, the swept area (A) is determined using Equation (2) [22].

$$A = \frac{2P_a}{\rho V_{max}^3} \quad (2)$$

where P is the wind power (watts), ρ is the air density (kg/m^3), A represents the blade swept area (m^2), and V is the wind speed (m/s) [22].

Based on the calculations, the swept area was found to be 50.2 m^2 , representing the operational area of the blades exposed to the wind flow. This area greatly influences the potential power that can be captured.

Table 1. Parameter 1 taper dan taperless blade design

Type of turbine	Efficiency (%)				
	Blade	Generator	Controller	Transmission	System
Taperless	40	90	90	90	29
Taper	40	90	90	90	29
Taperless Flat	40	90	90	90	29

Table 2. Operational characteristics of taper blade – parameter 1

Type of turbine	Electrical energy capacity (kWh)	Wind Energy (kW)	Vmax (m/s)	A (m ²)	Radius (m)
Taperless	6545	2256	9	50.2	4
Taper	6545	2256	9	50.2	4
Taperless Flat	6545	2256	9	50.2	4

Parameter 2 covers the geometric design aspects of the blades, including variations in blade configurations such as taperless, tapered, and taperless flat. Each design variation was analyzed based on simulation results using QBlade software to evaluate aerodynamic performance. The simulation results for each design using consistent variables are presented in Tables 1 and 2. The wind energy capacity was determined based on the energy demand in the Labuhan Jukung Beach area, Pesisir Tengah Subdistrict, Pesisir Barat Regency. According to data from the BPS, there are 595 households using electricity from Perusahaan Listrik Negara (PLN), with an average daily consumption of 11 kWh. Therefore, the total electricity demand in this area reaches 6545 kWh per day [1].

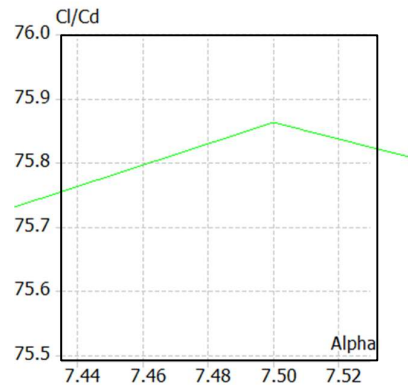


Figure 1. Cl/Cd max

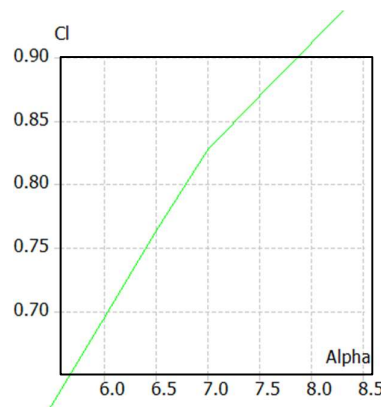


Figure 2. Cl and alpha value

The blade efficiency is set at 40%, while the efficiencies of the generator, controller, and transmission are each 90%, based on Betz's theory (which states that blade efficiency cannot exceed 59%). The total system efficiency, calculated as the product of all component efficiencies, is 29%. The wind energy (kinetic energy) is obtained by dividing the planned energy capacity by the system efficiency, resulting in a value of 2256 kW. The maximum wind speed (V_{max}) recorded from 2018 to 2022 is 9 m/s. The blade swept area (A) is 50.2 m². The assumption of a 40% blade efficiency and 90% efficiency for other system components (generator, controller, and transmission) is based on widely accepted practical values found in the literature for small-to medium-scale wind turbine systems operating under optimal conditions [20], [21]. These efficiency levels are consistent with the theoretical Betz limit of 59.3% and reflect realistic performance under nominal load scenarios. The maximum wind speed of 9 m/s, derived from ECMWF data for the 2018–2022 period, represents the highest typical wind condition observed at the study site and provides a reasonable upper bound for performance simulation. The use of fixed parameters in this context ensures consistency across the comparative analysis of blade geometries within a controlled simulation environment. Rather than serving as limitations, these assumptions form a foundational reference point for evaluating aerodynamic performance and system sizing. Additionally, these parameters create opportunities for future investigations involving dynamic modeling and parameter variation to further enrich the technical depth of subsequent development stages.

Next, an analysis was conducted using Xfoil direct foil analysis in QBlade software to obtain Parameter 2, which is visualized in a lift-to-drag ratio (Cl/Cd) graph and a Cl vs. angle of attack (Alpha) graph, using the NACA 0012 airfoil. The results are shown in Figure 1 and Figure 2. These parameters were then used in calculations presented in Table 3, which summarizes the characteristics of each blade type based on the airfoil used.

Table 3. Parameter 2 – taper and taperless blade design

Type of turbine	TSR	Airfoil	Number of blades	Chord length	Cl/Cd Max	Alpha	Cl
Taperless	7	NACA 0012	3	0.25	75.86	7.5	0.87
Taper	7	NACA 0012	3	75.86	7.5	0.87	7
Taperless flat	7	NACA 0012	3	0.25	75.86	7.5	0.87

Based on Table 3, most variables remain consistent, except for the chord length. The taper blade features a chord length that gradually narrows toward the blade tip. The maximum Cl/Cd ratio is recorded at 75.86, representing the highest lift-to-drag ratio achieved by the NACA 0012 airfoil. The angle of attack (Alpha) is 7.5°, and the lift coefficient (Cl) was obtained through simulation using QBlade software.

These simulation results are presented in graphical form to facilitate the identification of these variables. Once Parameters 1 and 2 are calculated using several equations, the next step is to develop Parameter 3, which involves designing the blade geometry. The parameter 3 table includes blade elements, with a blade radius of 4 meters and a TSR of 7. The flow angle (ϕ) is calculated using equation (3) [1].

$$\phi = \frac{2}{3} \tan^{-1} \left(\frac{1}{\lambda r} \right) \quad (3)$$

Meanwhile, the twist angle (β) is calculated using equation (4) [1].

$$\beta = \phi - \alpha \quad (4)$$

Linear twist is obtained by linearizing the twist angle with respect to the blade radius. The calculation results for parameter 3 are presented in Tables 4, 5, and 6.

Table 4. Parameter 3 – taperless blade geometry

Element	Radius (m)	Partial TSR	Flow angle	Twist angle	Twist 75%	Linear twist	Chord length (m)
0	0.2	0.35	47.14	39.64		6.08	0.25
1	0.58	1.02	29.72	22.22		5.22	0.25
2	0.96	1.68	20.51	13.01		4.35	0.25
3	1.34	2.35	15.40	7.90		3.49	0.25
4	1.72	3.01	12.25	4.75		2.63	0.25
5	2.1	3.68	10.15	2.65		1.76	0.25
6	2.48	4.34	8.65	1.15		0.90	0.25
7	2.86	5.01	7.53	0.03	0.03	0.03	0.25
8	3.24	5.67	6.67	-0.83	-0.83	-0.83	0.25
9	3.62	6.34	5.98	-1.52	-1.52	-1.70	0.25
10	4	7.00	5.42	-2.08	-2.08	-2.56	0.25

Based on Tables 4, 5, and 6, most variables remain consistent; however, there are notable differences in the twist angle column for the parameter 3 of the taperless flat blade, where no twist angle is present due to its straight, untwisted blade design.

Table 5. Parameter 3 – taper blade geometry

Element	Radius (m)	Partial TSR	Flow angle	Twist angle	Linear Twist	Chord length (m)	Chord length at 75%	Linear chord length (m)
0	0.2	0.35	47.14	39.64	6.08	3.494		0.395
1	0.58	1.015	29.72	22.22	5.22	1.205		0.366
2	0.96	1.68	20.51	13.01	4.35	0.728		0.338
3	1.34	2.345	15.40	7.90	3.49	0.521		0.309
4	1.72	3.01	12.25	4.75	2.63	0.406		0.280
5	2.1	3.675	10.15	2.65	1.76	0.333		0.252
6	2.48	4.34	8.65	1.15	0.90	0.282		0.223
7	2.86	5.005	7.53	0.03	0.03	0.244	0.244	0.194
8	3.24	5.67	6.67	-0.83	-0.83	0.216	0.216	0.166
9	3.62	6.335	5.98	-1.52	-1.70	0.193		0.137
10	4	7	5.42	-2.08	-2.56	0.175		0.108

Another difference appears in the chord length column. For the taperless blade, the chord length remains constant at 0.25 meters from the root to the tip. In contrast, the taper blade features a chord length that gradually decreases from root to tip. As a result, additional calculations are required to determine the chord length at 75% of the blade length, as well as to develop the linear chord distribution, which served as geometric input for the QBlade software.

Table 6. Parameter 3 – taperless flate blade

Element	Radius (m)	Partial TSR	Flow angle	Chord length (m)
0	0.2	0.35	47.14	0.25
1	0.58	1.02	29.72	0.25
2	0.96	1.68	20.51	0.25
3	1.34	2.35	15.40	0.25
4	1.72	3.01	12.25	0.25
5	2.1	3.68	10.15	0.25
6	2.48	4.34	8.65	0.25
7	2.86	5.01	7.53	0.25
8	3.24	5.67	6.67	0.25
9	3.62	6.34	5.98	0.25
10	4	7.00	5.42	0.25

Previously, for the taperless blade, the linear twist was obtained by linearizing the twist angle with respect to the blade radius (r) through a plotted graph. In the case of the taper blade, in addition to the twist angle linearization, it is also necessary to linearize the chord length relative to the radius, as shown in Figures 3 and 4. In Figure 3, linearization was performed to determine the linear twist, resulting in the equation: $y = -2.2749x + 6.5389$. The blue dots on the graph represent the linearized relationship between the twist angle and the radius (r), while the orange dots represent the linearization at 75% of the blade length.

In Figure 4, linearization was conducted to determine the linear chord length for the taper blade, resulting in the equation: $y = -0.0754x + 0.46$. The blue dots indicate the relationship between chord length and radius (r), while the orange dots represent the chord length at 75% of the blade span.

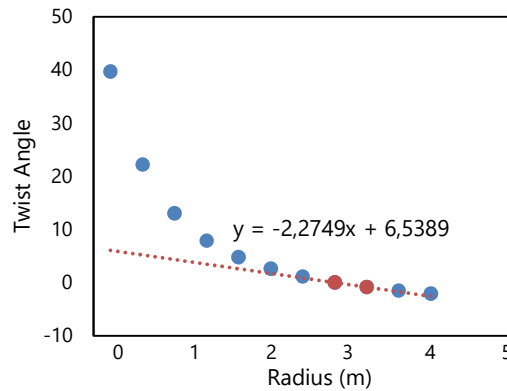


Figure 3. Twist angle as a function of blade radius (r)

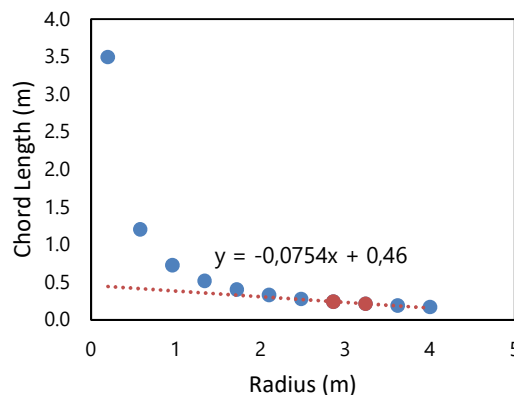


Figure 4. Chord length as a function of blade radius (r)

Based on these findings, the main difference between Parameter 3 of the taper and taperless blades lies in the shape and variation of the chord length, which is adjusted according to the blade type. To further analyze these differences, simulations were carried out using QBlade software, and the blade design results for the taperless and taper configurations are shown in Figures 5 and 6, respectively. The simulations confirm that the taperless blade maintains a constant chord length from root to tip, whereas the taper blade features a chord length that gradually narrows toward the tip.

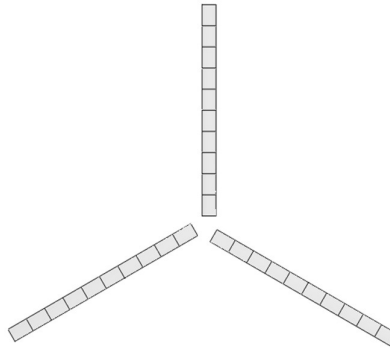


Figure 5. Taperless blade

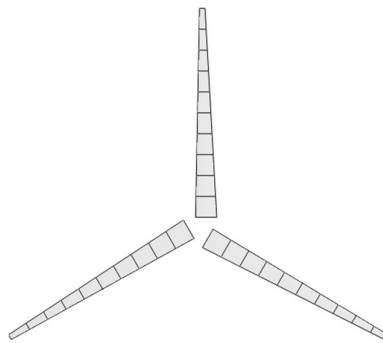


Figure 6. Taper blade

3.2. Analysis of Results and QBlade Simulation Output

The analysis of calculation results and QBlade simulation is based on the previous computations, supported by a review of relevant literature, to compare the performance of horizontal-axis wind turbine blades with taperless, taper, and taperless flat designs. The comparison results are presented in Tables 7 and 8, where differences in power coefficient (C_p), thrust coefficient (C_t), power (P), and torque (T) with respect to TSR are identified for each blade type, particularly between taperless and taper blades.

The values for each variable were obtained by exporting the simulation graphs from QBlade and then converted into datasets to generate comparison graphs. These are illustrated in:

- a) Figure 7: comparison of C_p vs. TSR
- b) Figure 8: comparison of C_t vs. TSR
- c) Figure 9: comparison of torque (T) vs. TSR
- d) Figure 10: comparison of power output (P) vs. TSR

Table 7. Power and thrust coefficient comparison of taperless, taper, and taperless flat wind turbine blades

TSR	Cp			Ct		
	Taperless	Taperless Flat	Taper	Taperless	Taperless Flat	Taper
1	0.001	0.001	0.001	0.11	0.11	0.099
2	0.005	0.005	0.004	0.14	0.12	0.12
3	0.067	0.074	0.054	0.22	0.24	0.18
4	0.270	0.256	0.189	0.44	0.33	0.32
5	0.408	0.377	0.295	0.63	0.52	0.46
6	0.466	0.449	0.440	0.77	0.68	0.62
7	0.470	0.480	0.469	0.88	0.80	0.73

Table 8. Comparison of power output torque for taperless, taper, and taperless flat wind turbine blades

TSR	P (kWh)			T (Nm)		
	Taperless	Taperless flat	Taper	Taperless	Taperless flat	Taper
1	1.1	0.7	1.0	14.2	13	14
2	3.6	3.6	3.2	24	33	22
3	50	44	32	223	273	156
4	199	137	125	672	638	445
5	301	203	218	814	752	614
6	344	243	288	775	746	668
7	347	264	331	669	640	690

Based on Figure 7, a comparison of the power coefficient (C_p) against the TSR for the three blade types is presented. It can be observed that at TSR values between 1 and 2, all blade types exhibit very low C_p values, indicating that at low TSR, the blades are not yet operating efficiently. This is due to the insufficient wind speed to optimally rotate the turbine. Between TSR 4 and 6, the taperless blade shows better efficiency compared to the taper blade, while the taperless flat blade has slightly lower efficiency than the taperless blade. At TSR 7, all three blades reach similar C_p values: 47% for taperless, 46% for taper, and 48% for taperless flat.

These values approach the theoretical Betz Limit, which states that the maximum practical efficiency of a wind turbine is around 59.3%, though in real-world conditions, turbines typically achieve a C_p of about 45–50%. The C_p value served as an indicator of the blade's ability to extract energy from the wind. It can also be interpreted as the ratio between the generator's power output and the available wind power, making it a key measure of wind turbine efficiency.

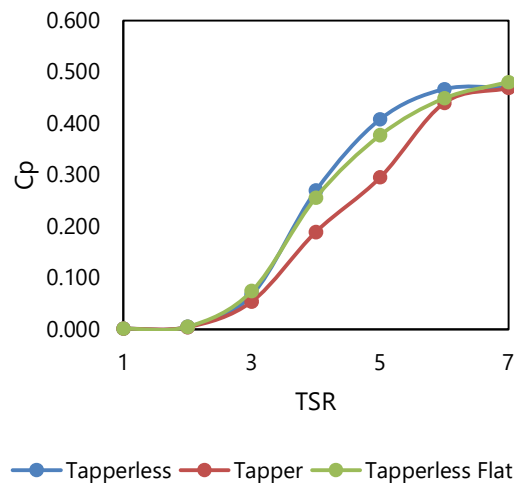


Figure 7. Power coefficient (C_p) comparison of taperless, taper, and taperless flat wind turbine blades

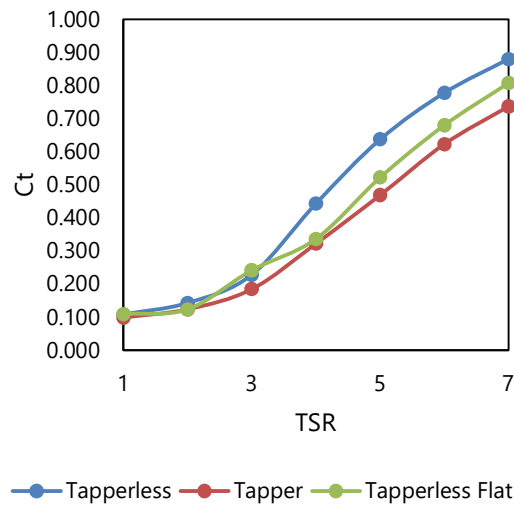


Figure 8. Thrust coefficient (C_t) comparison of taperless, taper, and taperless flat wind turbine blades

Based on Figure 8, the comparison of the thrust coefficient (C_t) versus TSR for the three types of turbine blades is presented. Within the TSR range of 1–2, all blade types exhibit very low C_t values, indicating that the generated thrust force is still minimal due to the low relative wind speed. As TSR increases to the range of 2–5, the C_t values begin to rise for all blade types. In this range, the taperless and taperless flat designs demonstrate better thrust performance compared to the taper blade.

At TSR 7, the taperless blade achieves the highest C_t value, at 0.880, followed by the taperless flat blade at 0.808, and the taper blade at 0.737. These findings indicate that untapered blade designs (taperless), especially those incorporating a twist angle, are more effective at capturing thrust force from the wind flow. The C_t value reflects the magnitude of thrust force generated by the wind turbine. The greater the thrust captured by the blades, the higher the torque produced, which ultimately contributes to improved overall power output of the wind turbine.

Based on Figure 9, the comparison of torque (T) in Newton-meters (Nm) versus TSR is presented for the three wind turbine blade designs. At TSR values of 1–2, all blade types generate very low torque, which is attributed to the low wind speed, preventing the blades from producing significant rotational force.

As TSR increases to the 4–5 range, torque rises substantially. The taperless blade demonstrates the best performance, reaching 814 Nm, followed by the taperless flat blade at 752 Nm, and the taper blade at 614 Nm. This indicates that at moderate TSR values, the taperless design is more efficient in generating torque.

However, at TSR 7, both the taperless and taperless flat blades experience a decrease in torque to 669 Nm and 640 Nm, respectively. In contrast, the taper blade shows an increase in torque to 690 Nm. The decline in torque for the taperless designs is likely due to aerodynamic instability caused by the higher blade rotational speed, which reduces the blades' ability to efficiently capture wind energy.

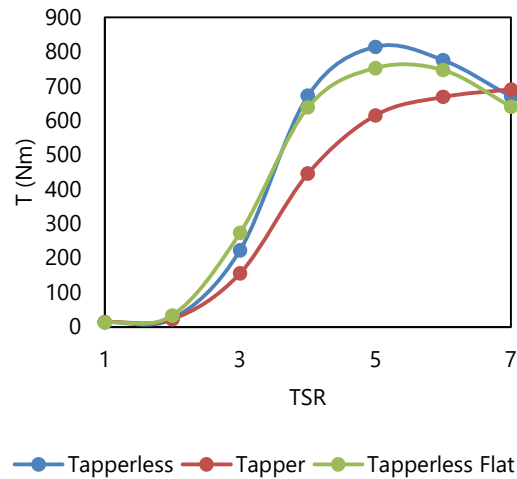


Figure 9. Comparison of torque (T) in newton-meters for taperless, taper, and taperless flat blades

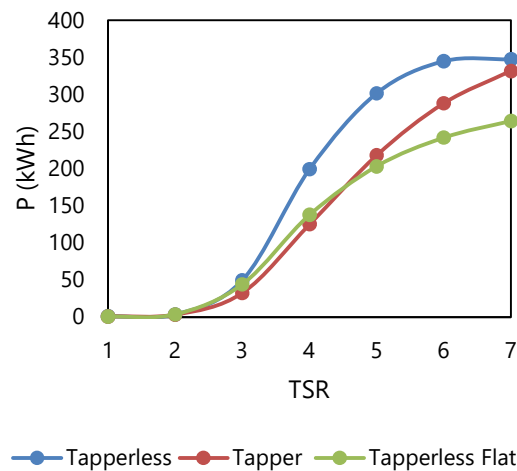


Figure 10. Power output (P) comparison in kwh for taperless, taper, and taperless flat wind turbine blades

Overall, although the taperless blade demonstrates the highest torque performance at moderate TSR levels, its performance tends to decline at higher TSR, approaching that of the taper blade. This indicates that in terms of consistency, the taper blade can produce more stable torque output. Torque is the rotational force generated by the blades when exposed to wind flow. It plays a crucial role because it directly influences the amount of mechanical energy that can be converted into electrical energy by the wind turbine generator.

Based on Figure 10, a comparison of power output (P) in kilowatt-hours (kWh) versus TSR is presented for the three wind turbine blade designs. At TSR values of 1–2, the power output of all blade types remains very low. This is due to insufficient wind speed to generate significant electrical energy. At higher TSR values (e.g., TSR 7), the taperless and taperless-flat blades exhibit a slight decline in torque, while the taper blade maintains or slightly increases torque. This behavior is consistent with known aerodynamic effects, where higher rotational speeds can lead to reduced relative wind angle, flow separation, or stall near the blade root or tip, thereby decreasing effective torque output [18], [21]. Moreover, the simpler geometry of taperless blades, while advantageous for manufacturing, may result in higher thrust loads at the tips under high TSR conditions, which can compromise aerodynamic stability [23]. Tapered blades, with their narrower tips, are structurally more stable at high rotational speeds and may better resist dynamic loading and vibration [24].

A noticeable increase in power output occurs between TSR 2–5. At TSR 5, the taperless blade produces the highest output at 301 kWh, followed by the taper blade at 218 kWh, and the taperless flat blade at 203 kWh. This indicates that the taperless blade is more effective in capturing and converting wind energy under moderate TSR conditions.

At TSR 7, all blades reach their maximum power output. The taperless blade continues to perform best, generating 347 kWh. Meanwhile, the taper blade produces slightly less at 331 kWh, and the taperless flat blade yields 264 kWh.

These results suggest that the taperless design, particularly with an optimal twist angle, can generate higher electrical output compared to the other designs. In this context, power (P) refers to the electrical energy generated by the wind turbine, measured in kilowatt-hours (kWh), and served as a key indicator of wind turbine energy conversion performance.

3.3. Analysis of Required Turbine Units: Taperless, Taper, and Taperless Flat Designs

In this study, the analysis and determination of the required number of wind turbines using taperless, taper, and taperless flat blade designs for application in the Labuhan Jukung Beach area were based on several key considerations. These include the local wind speed at Labuhan Jukung, the power coefficient (C_p), thrust coefficient (C_t), torque (T in Nm), and power output (P in kWh) generated by each blade type. The comparative performance results of the three blade designs are summarized in Table 9 as follows.

Table 9. Performance and wind energy conversion results of taperless, taper, and taperless flat wind turbine blades

Parameter	Taperless	Taperless flat	Taper
C_p	47%	48%	46%
C_t	0.88	0.80	0.73
T (Nm)	814	640	690
P (kWh)	347	264	331

Based on the research results, the power coefficient (C_p) for the taperless and taperless flat blades across TSR values 1 to 7 reached relatively high values of 47% and 48%, respectively, compared to the taper blade, which was slightly lower at 46%. The thrust coefficient (C_t) of the taperless blade was also higher, reaching 0.880, compared to 0.737 for the taper blade and 0.808 for the taperless flat blade. In terms of torque (T), the taperless blade achieved the highest maximum torque of 814 Nm, outperforming the taper blade (690 Nm) and the taperless flat blade (640 Nm). For power output (P), the taperless blade again showed superior performance, producing up to 347 kWh, while the taper blade produced 331 kWh and the taperless flat blade only 264 kWh. Following the comparison of all three blade types, the next step is to determine the number of turbine units required to meet the daily electricity consumption needs in Pesisir Tengah Subdistrict, which is presented in Table 10 below.

To analyze the number of turbines required, the calculation begins with the daily electrical power output of each blade type. A turbine equipped with a taperless blade can produce 347 kWh per day. Therefore, to meet the daily electricity consumption of 6545 kWh in Pesisir Utara Subdistrict, approximately 19 taperless turbines are needed. A taper blade turbine generates 331 kWh per day, which means 20 taper turbines are required to meet the same daily energy demand. Meanwhile, a turbine with a taperless flat blade produces 264 kWh per day. Thus, to fulfill the same daily electricity requirement of 6545 kWh, a total of 25 taperless flat blade turbines would be necessary.

In the design of wind turbine blades, several factors influence the overall efficiency level. One of the main factors is the complexity of the blade design itself. The taper blade design tends to be more complex due to its gradually narrowing shape from root to tip. This variation in size requires more intricate aerodynamic calculations and a higher degree of precision during the manufacturing process. As a result, production costs and processing time are generally higher, and the process demands skilled labor. In contrast, the taperless blade features a

simpler geometry, with a relatively constant chord width from root to tip. Its simplified geometry improves fabrication efficiency and reduces production costs.

Based on the power output analysis, it is evident that the number of turbines required to meet daily electricity demand varies depending on the blade type used. The taperless blade generally requires fewer turbine units than the taper blade to generate the same amount of electricity, due to its higher efficiency under moderate wind conditions. Blade performance characteristics significantly influence their suitability for specific wind conditions. The taperless blade proves to be more effective when applied in regions with moderate wind speeds, making it a more appropriate choice for such environments.

Table 10. Number of turbines required for taperless, taper, and taperless flat blades

Type of turbine	Power output per turbine (kWh/day)	Number of turbines required	Total electricity consumption (kWh/day)
Taperless	347	19	6545
Taper	331	20	6545
Taperless Flat	264	25	6545

Its design allows the blade cross-section to receive wind flow more evenly, enabling the blade to start rotating earlier and generate power more quickly. However, at high wind speeds, this blade tends to be less stable and may experience reduced efficiency due to aerodynamic instability. In contrast, the taper blade, with its narrower tip, is more suitable for high wind regions, as only a small portion of the blade tip is directly exposed to the wind flow. This makes the blade more stable at high rotational speeds and better suited for high-speed turbine systems. Therefore, the selection of blade type should not be based solely on power efficiency, but also must consider local wind conditions, production costs, and the intended application of the wind turbine system as a whole.

Based on the analysis results, it can be concluded that the most suitable wind turbine blade type with a NACA 0012 airfoil profile for the study location is the taperless blade. This is due to its ability to generate optimal power output under moderate wind speed conditions. A location such as Labuhan Jukung Beach, which experiences a maximum wind speed (V_{max}) of up to 9 m/s, is considered ideal for the application of taperless blades.

Under these conditions, a taperless blade can produce 347.6 kWh of electricity per turbine per day. Considering the daily electricity consumption in Pesisir Utara Subdistrict, Pesisir Barat Regency, which reaches 6,545 kWh, approximately 19 turbines are required to meet this demand.

The high wind speeds in this area are also influenced by geographical factors, such as the presence of sea breezes, which are common in coastal and island regions adjacent to open seas. This phenomenon gives locations like Labuhan Jukung Beach a consistent and relatively strong wind potential, making them suitable for wind-based electricity generator.

Therefore, the selection of the taperless blade is based not only on its aerodynamic efficiency but also on the compatibility of its design characteristics with the local microclimate and geographic conditions. Although the simulation results presented in this study provide a structured comparison of tapered, taperless, and flat taperless blade designs, it is important to recognize that these results are derived from ideal and steady state wind conditions within the QBlade environment. As such, several sources of uncertainty, including variations in wind direction, turbulence intensity, and model simplifications, may influence real-world performance but are not explicitly captured in the simulation.

In addition to its competitive aerodynamic performance, the taperless blade design offers a significant practical advantage in terms of manufacturability due to its uniform geometry from root to tip. This structural simplicity facilitates easier fabrication, reduces production time, and lowers material and labor costs—factors that are especially important for the deployment of renewable energy systems in coastal or remote regions. Although the taper blade demonstrated slightly higher torque at the maximum TSR (≈ 7), the difference is relatively minor and less critical given that the local wind speeds at the study site predominantly range from 2.5 to 6 m/s.

Therefore, the simplicity and cost-effectiveness of the taperless blade design make it a more feasible and scalable solution for real-world implementation in the specified location.

4. Conclusion

Based on the analysis and calculations conducted, the following conclusions can be drawn. Performance Comparison: The comparison between taperless, taper, and taperless flat blade designs shows that the taperless blade has superior performance in terms of power coefficient (C_p) and thrust coefficient (C_t), with values of 47% and 0.88, respectively. In terms of torque (T), the taperless blade also demonstrates the highest maximum performance at 814 Nm, which is greater than both taper blade (690 Nm) and taperless flat blade. Energy Conversion Efficiency: In converting wind energy into electrical energy, the taperless blade again delivers the highest performance, producing a maximum power output of 347 kWh. In comparison, the taper blade generates 331 kWh, while the taperless flat blade produces 264 kWh. Suitability for Local Wind Conditions: The taperless blade proves to be optimal for moderate wind speeds, such as those at Labuhan Jukung Beach, where the maximum recorded wind speed is 9 m/s. At this speed, a single taperless turbine can produce up to 347.6 kWh per day. Therefore, to meet the daily electricity consumption of 6,545 kWh in Pesisir Utara Subdistrict, Pesisir Barat Regency, approximately 19 taperless wind turbines are required.

The results of this study indicate that taperless blade configurations offer significant potential for practical application in regions characterized by moderate wind conditions, such as coastal areas in Indonesia. The implementation of small-to medium-scale wind turbine systems using taperless blades can provide a viable solution to address energy access challenges, particularly in remote or underserved communities with limited grid connectivity. Integrating such systems into hybrid renewable energy frameworks—such as wind-solar combinations—can further enhance energy security and sustainability. It is recommended that regional energy planners and policymakers consider the deployment of taperless-blade turbines as part of decentralized energy development strategies, contributing to the achievement of national renewable energy targets and climate resilience initiatives.

Despite the promising results, this study has several limitations that require further investigation. The reliance on secondary wind data from ECMWF, while suitable for large-scale assessments, overlooks localized turbulence, topographic influences, and diurnal wind variations that can significantly impact actual turbine performance. Moreover, the analysis focused solely on aerodynamic performance under steady-state conditions, without addressing structural dynamics, material fatigue, or noise emissions. To build on these findings, future research should incorporate experimental validation through field testing, employ Computational Fluid Dynamics (CFD) integrated with Fluid-Structure Interaction (FSI) modeling, and include comprehensive techno-economic assessments to evaluate real-world feasibility. Additionally, exploring adaptive blade designs, advanced control strategies, and stochastic approaches such as Monte Carlo simulations or parameter sensitivity analysis is recommended to better account for uncertainty and enhance the robustness and adaptability of the system across diverse environmental conditions.

5. Acknowledgments

-

6. References

- [1] A. Nuraini, C. S. Abadi, and Fachruddin, "Analisis perbandingan bilah turbin angin jenis taper dengan taperless pada turbin angin skala mikro di PT. lentera bumi nusantara," *Prosiding Seminar Nasional Teknik Mesin Politeknik Negeri Jakarta*, pp. 138–146, 2019.
- [2] P. Pratiwi and F. Yurian, "Design of a semi-inverse taper horizontal blade wind turbine and its potential use at gajah beach padang," *J. Tek. Mesin*, vol. 11, no. 1, pp. 74–79, 2021, doi: 10.21063/jtm.2021.v11.i1.74-79.

- [3] Y. Ardiansyah, I. N. Gusniar, and O. Oleh, "Perancangan bilah tipe taperless dengan menggunakan airfoil S2046," *METTEK*, vol. 8, no. 2, pp. 65-73, 2022, doi: 10.24843/mettek.2022.v08.i02.p01.
- [4] M. Dreila, "XFOIL: an analysis and design system for low reynolds number airfoils," *LNME*, vol 54, pp. 1–12, 1989, , doi: 10.1007/978-3-642-84010-4_1.
- [5] M. Kamran and M. R. Fazal, "Renewable energy conversion systems," *Amsterdam: Elsevier*, 2021, doi: 10.1016/C2019-0-05410-6.
- [6] H. S. Tira and M. P. Zulfikar, "Design of tapered wind turbine using various NACA 24112 airfoils in Semayan Village Central Lombok Regency," *Machine*, vol. 10, no. 2, pp. 41-26, 2024, doi: 10.33019/jm.v10i2.4704.
- [7] A. Akmal, M. Perdana, R. Saputra, H. Fahmi, and S. Sulaiman, "Analisa daya turbin angin sumbu horizontal bladetaperless berbahan komposit hybrid dengan airfoilblade Tipe NACA," *JREM*, vol. 2, no. 2, pp. 145–153, 2022, doi: 10.26760/JREM.v2i2.145.
- [8] M. F. Wicaksono and D. B. Saefudin, "Pemilihan bilah turbin angin sumbu horizontal model air foil taperless dan untwisted," *JPTI*, vol. 3, no. 10, pp. 439–446, 2023, doi: 10.52436/1.jpti.334.
- [9] S. A. H. Roslan, Z. A. Rasid, and A. K. A. M. Ehsan, "The aerodynamic performance of the small-scale wind turbine blade with NACA0012 Airfoil," *CFD Letters*, vol. 14, no. 10, pp. 87–98, 2022, doi: 10.37934/cfdl.14.10.8798.
- [10] National Renewable Energy Laboratory (NREL), "Wind resource classification," *U.S. Department of Energy*. [Online]. Available: <https://www.nrel.gov>
- [11] European Centre for Medium-Range Weather Forecasts, "ERA5 wind speed dataset 2017–2022," *ECMWF*. [Online]. Available: <https://www.ecmwf.int>
- [12] T. Ackermann, "Wind power in power systems 2nd ed.," *John Wiley & Sons Ltd*, 2012.
- [13] Badan Pusat Statistik Kabupaten Pesisir Barat, "Statistik daerah kabupaten pesisir barat 2023," *BPS*, 2023. [Online]. Available: <https://pesisirbaratkab.bps.go.id>
- [14] I. N. Wani *et al.*, "Design & analysis of NACA 0012 airfoil with circular dent of 30 mm depth on upper surface," *Mater Today Proc*, 2023, doi: <https://doi.org/10.1016/j.matpr.2023.05.013>.
- [15] I. H. Abbott and A. E. V. Doenhoff, "Theory of wing sections: including a summary of airfoil data", *New York: Dover Publications inc*, 1959.
- [16] M. Madi, T. Tuswan, I. D. Arirohman, and A. Ismali, "Comparative analysis of taper and taperless blade design for ocean wind turbines in ciheras coastline, west java," *Kapal*, vol. 18, no. 1, pp. 8–17, 2021, doi: 10.14710/kapal.v18i1.32486.
- [17] D. Marten, J. Wendler, G. Pechlivanoglou, C.N. Nayeri, and C.O. Paschereit, "QBLADE: an open source tool for design and simulation of horizontal and vertical axis wind turbines," *IJETAE*, vol 3, no. 3, pp. 264-269, 2013.
- [18] T. Burton, N. Jenkins, D. Sharpe, and E. Bossanyi, "Wind energy handbook 2nd ed.," in *Wind Energy Chichester: John Wiley & Sons*, 2011, doi: 10.1002/9781119992714.
- [19] J. R. Horton, "An introduction to dynamic meteorology," *Elsevier Academic Press*, 2004.
- [20] A. Betz, "Wind-Energie und Ihre Ausnutzung durch Windmühlen," *Göttingen, Germany: Vandenhoeck & Ruprecht*, 1926.
- [21] E. Hau, "Wind turbines: fundamentals, technologies, application, economics (3rd ed.)," *Berlin, Jerman: Springer*, 2013.
- [22] R. B. Stull, "An introduction to boundary layer meteorology," *Netherlands: Springer*, 1988.
- [23] R. Gasch and J. Twele, "Wind power plants: fundamentals, design, construction and operation, 3rd ed.," *Berlin, Germany: Springer*, 2012.
- [24] M. M. Hand *et al.*, "Unsteady aerodynamics experiment phase vi: wind tunnel test configurations and available data campaigns," *Colorado*, 2001, doi: 10.2172/15000240, [Online]. Available: <http://www.osti.gov/biblio/15000240>.